Strong absorption and selective thermal emission from a midinfrared metamaterial

J. A. Mason, S. Smith, and D. Wasserman[a)]
Department of Physics, University of Massachusetts Lowell, One University Avenue, Lowell, Massachusetts 01854, USA

(Received 22 March 2011; accepted 27 May 2011; published online 15 June 2011)

We demonstrate thin-film metamaterials with resonances in the midinfrared (mid-IR) wavelength range. Our structures are numerically modeled and experimentally characterized by reflection and angularly resolved thermal emission spectroscopy. We demonstrate strong and controllable absorption resonances across the mid-IR wavelength range. In addition, the polarized thermal emission from these samples is shown to be highly selective and largely independent of emission angles from normal to 45°. Experimental results are compared to numerical models with excellent agreement. Such structures hold promise for large-area, low-cost metamaterial coatings for control of gray- or black-body thermal signatures, as well as for possible mid-IR sensing applications. © *2011 American Institute of Physics*. [doi:10.1063/1.3600779]

The emergence of the field of metamaterials has led to the development of artificial materials with predefined optical properties not obtainable in nature. The potential applications for metamaterials are numerous with the most commonly cited being the development of optical cloaks[1,2] and superlenses.[3–6] In the midinfrared (mid-IR) wavelength range (2–30 μm), where all finite temperature biological materials and mechanical objects emit thermal radiation, this ability to tailor materials' optical properties has potentially significant implications for sensing, defense, and security applications.

In this work, we demonstrate selective thermal emission from metamaterial films with controllable resonances in the mid-IR spectral range. Our structures are characterized by reflectivity and angularly dependent emissivity measurements, and are simulated using commercial FEM software. The metamaterials demonstrated here are easily fabricated and can be removed from their carrier substrate, giving a thin-film mid-IR metamaterial wall-paper for coating thermal emitters.

Fundamentally, the basis for selective thermal emission lies the ability to control a material's absorbtivity, $\alpha(\lambda)$, which, by Kirchoff's Law, is equivalent to controlling the material emissivity, $\varepsilon(\lambda)$.[7] For any material, then, we can experimentally determine emissivity by accounting for all of the light not absorbed by the material (reflected, scattered, and transmitted). A material with subwavelength surface roughness and geometry can be treated as a homogeneous material, thus removing the scattering term.[8] With the inclusion of an optically thick layer of metal as the material ground plane (preventing transmission), Kirchoff's Law reduces to the simplified $\alpha(\lambda)=\varepsilon(\lambda)=1-r(\lambda)$, where $r(\lambda)$ is the wavelength-dependent reflectivity.

Perfect absorbers and selective emitters based on plasmonic and phononic metamaterials have been demonstrated recently at IR frequencies.[9–13] Similar structures have also been proposed and numerically and analytically characterized at terahertz and near-IR frequencies.[14,15] Our structures are quite similar to those described in the references above,[9,10,14] and consist of a three layer system as follows: an optically thick layer of gold (Au) below a layer of spin-on-glass (SOG) into which is integrated a periodic array of Au strips. While earlier work utilized circular plasmonic "pucks," giving a polarization insensitive optical response, our one-dimensional stripes will result in strong absorption signatures for only TM-polarized light (as shown in Fig. 1). Despite this, the underlying physics of the structures remains similar. The distinctive optical characteristics of our structures can be qualitatively understood as follows: for TM-polarized light, the stripes act as optical antennas, coupling in incident radiation with a resonance based upon the stripe width (as well as the surrounding dielectric). The incident radiation couples strongly to the magnetic moment created by the antiparallel surface currents in the stripe and the metal ground plane. The confinement of electromagnetic energy in the dielectric spacer between the stripes and the ground plane results, ideally, for a dielectric spacer of the correct thickness, in 100% absorption. In Ref. 9, the absorption of energy occurs in the gold layers. For our structures, as we will show,

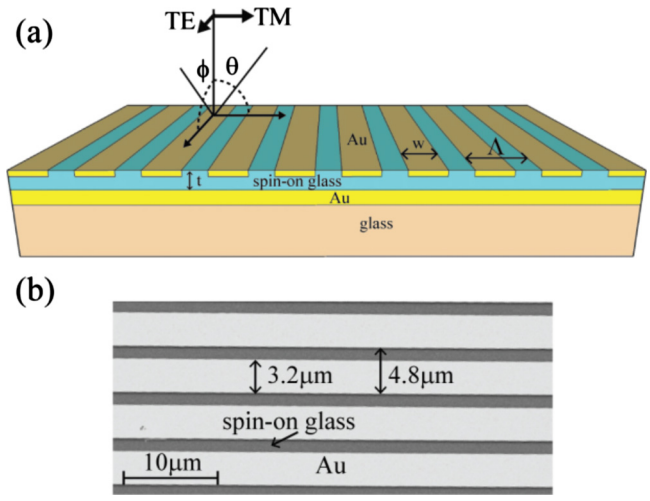

FIG. 1. (Color online) (a) Schematic of the mid-IR metamaterial absorber and (b) scanning electron micrograph of the sample.

[a)]Author to whom correspondence should be addressed. Electronic mail: daniel_wasserman@uml.edu.

absorption occurs in both the dielectric spacer and the Au layers.

A schematic of our sample structure, as well as a scanning electron micrograph of a representative sample is shown in Fig. 1. The structures are fabricated by first patterning the 50 nm thick Au stripes with periodicity $\Lambda = 4.8$ μm onto a sacrificial substrate. The SOG (Honeywell Accuglass 211) is then spun (thickness t=250 nm) above the Au stripes and cured, and subsequently coated with the thick (200 nm) Au layer. The sacrificial substrate is removed and the thin film attached to a glass slide, solid Au side down. Samples with stripe widths of w=1.9, 2.26, and 3.18 μm were fabricated and characterized.

Samples were first studied by reflection spectroscopy. Here, normally incident, polarized broadband mid-IR light from a Bruker V80 Fourier Transform Infrared (FTIR) spectrometer was focused onto the surface of the patterned material through a mid-IR beam splitter and the reflected light from the sample surface was collected by an external HgCdTe detector and normalized to the polarized reflection from a flat gold mirror. By Kirchoff's Law, dips in the reflection spectra, for wavelengths greater than the stripe periodicity, indicate coupling to absorption resonances.

Our samples were subsequently characterized by thermal emission spectroscopy. Here the patterned sample was heated to 160 °C using a custom-built hot-plate mounted on a rotational stage. The emission from the sample passes through a mid-IR polarizer, is spatially filtered to minimize the angular spread of the collected light, collimated with a ZnSe lens, and analyzed with the FTIR spectrometer. The collected spectra were compared to a calibrated blackbody source (Infrared Industries model 101C) at 160 °C. The background thermal emission of the experimental setup (without sample or heaters) was collected and subtracted from each spectrum (sample and calibrated blackbody). The background-corrected emission spectra from our samples are then normalized to the background-corrected blackbody source.

Our samples showed strong absorption resonances at wavelengths determined by the device stripe width, and not stripe periodicity, indicating that the observed resonances are localized to individual stripes [Fig. 2(b)]. For the device with 3.18 μm stripe widths, 100% absorption was achieved at a wavelength of 8 μm. In order to understand the nature of these absorption resonances, the optical properties of the SOG layer were obtained by broadband ellipsometry measurements, shown in Fig. 2(c). The SOG exhibits a number of absorption peaks, with the dominant peak at $\lambda \approx 9$ μm. A weaker SOG absorption is also seen at $\lambda \approx 7.85$ μm. For device geometries giving absorption resonances far from the 7.85 μm SOG absorption line, this feature appears as a dip in the normal incidence reflection spectra. However, for the w=3.18 μm stripes, where the geometric absorption resonance is well-aligned with the 7.85 μm material absorption line, a clear splitting is observed in the device reflection spectra giving a local increase in the device reflectivity at the material resonance, and suggesting a coupling between our device's geometric resonance and the material resonance in the SOG.

Our structures were numerically simulated with commercial FEM software,[16] using the experimentally determined SOG complex index of refraction. Reflectivity plots for our numerical models are shown in Fig. 2(a). The simulated data

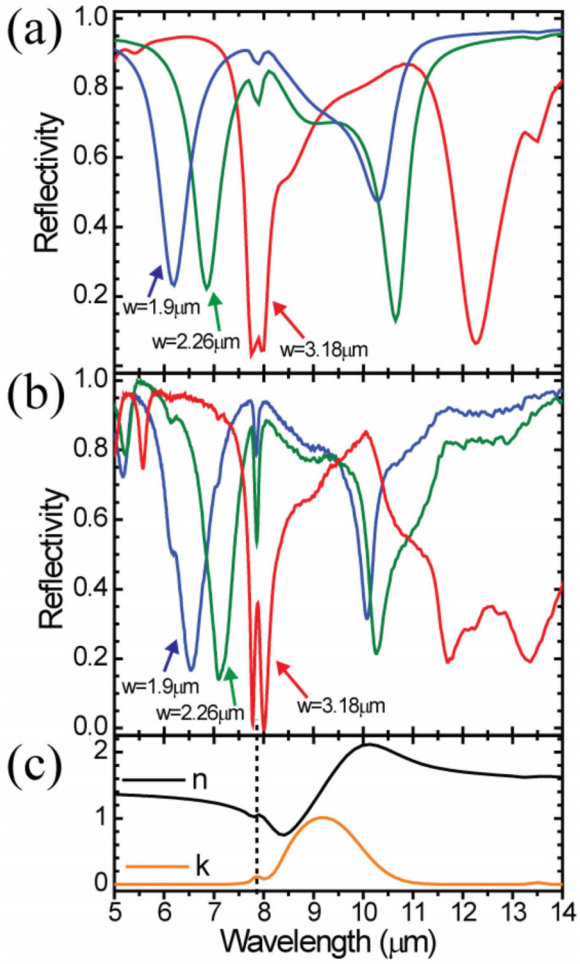

FIG. 2. (Color online) (a) Simulated and (b) experimental reflectivity from metamaterial absorbers for stripe widths of 1.9 μm, 2.26 μm, and 3.18 μm. Dashed circle shows broad material absorption not observed in the ellipsometry sample. (c) Experimentally determined real (n) and imaginary (k) components of the SOG refractive index.

shows excellent agreement with our experimental results, with the exception of the long-wavelength ($\lambda > 11$ μm) reflectivity of the w=3.18 μm sample, which displays a split reflectivity dip not seen in simulations or suggested by the SOG absorption data. This discrepancy may be a result of a shift in the SOG absorption due to the additional processing required for sample fabrication (but not for ellipsometry samples), and evidenced by the broad and weak absorption signal seen in the w=1.9 and w=2.26 μm data [dashed circle in Fig. 2(b)].

The demonstration of strong absorption in our samples should result in strongly selective emission at the absorption peaks upon sample heating. Figure 3 shows the background corrected and normalized emission spectrum from the w =3.18 μm structure, as well as the reflectivity from the same sample, for comparison. As expected, spectral dips in the sample's reflection spectrum are mirrored by peaks in the selective emission of the sample. It is important to note that although the emissivity rises above unity at resonance, we do not claim that our samples will emit more power, at certain wavelengths, than a blackbody at equivalent temperature. Such an anomaly has been noted in previous selective emission work,[17] and was eventually determined to be a result of localized heating of the selective emitter beyond the bulk

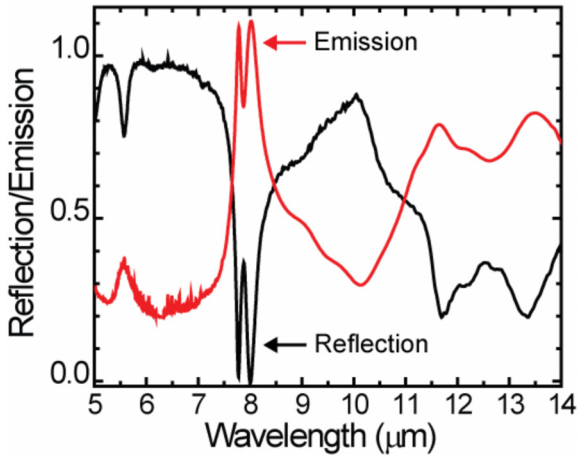

FIG. 3. (Color online) Reflectivity and emissivity of metamaterial absorber structures with stripe widths of 3.18 μm. Emission data were taken at 160 °C and normalized to a calibrated blackbody source at the same temperature.

material temperature.[18] As radiative emission away from the sample resonance is suppressed, the quenching of these radiative channels results in a localized heating of the thin metamaterial membrane. Because we measure sample temperature on the carrier substrate, and not the film itself, the substrate temperature is expected to underestimate the actual local temperature of the metamaterial film.

Finally, angular TM polarized emission from the surface of the heated sample (w=3.18 μm) was collected for emission angles between 0° and 45° in both the θ and φ directions [see Fig. 1(a)] in order to determine the angular dependence of thermal emission from our structures (Fig. 4). The contour data sets of Figs. 4(a)–4(c) are normalized (max =1) to better show the emission peak spectral position and

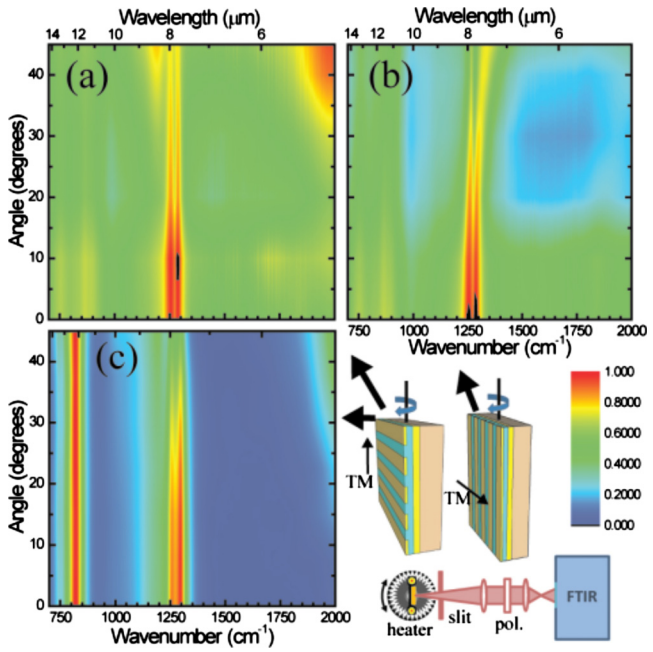

FIG. 4. (Color online) Normalized angular dependence of thermal emission from 3.18 μm stripe width metamaterial sample for rotations in (a) θ (experimental), (b) φ (experimental), and (c) θ (numerical, derived from reflectivity). (d) Schematic of experimental setups for data collected in [(a) and (b)].

relative intensity (compared to surface normal emission), as a function of emission angle.

In addition, the angular dependence of the sample reflectivity was numerically modeled for varying θ by changing the angular position of the simulated source boundary relative to the device interface. Reflectivity [r(λ)] was measured by comparing the total electromagnetic power flux across a boundary surrounding the illuminated structure to the total incident power and the resulting 1−r(λ) [effectively, $\alpha(\lambda)$] was plotted for angles θ=0°–45°. A strong selective emission is experimentally seen at λ ~ 8 μm, and its insensitivity to angle is in good agreement with both our numerical simulations and the results of Ref. 9. Slight spectral shifts in the selective emission peak can be seen for angled emission at higher φ, an effect also noted in Ref. 9.

In summary, we have designed, fabricated, and characterized thin-film mid-IR metamaterials with strong absorption resonances. The fabricated structures, as expected, demonstrate strongly selective polarized thermal emission at the designed wavelength. Our experimental results show excellent agreement to numerical simulations. In addition, we qualitatively determine the absorption/emission signals to be a result of both geometrical and material resonances. The development of lossless mid-IR transparent dielectric spacer layers will allow for structures with geometry-based perfect absorption resonances. Conversely, the strong spectral modulation from weak absorption resonances in the dielectric spacer layer suggests the potential of similar structures for mid-IR sensing applications. In total, the device geometries presented show significant potential for the further development of mid-IR metamaterial-based devices and thin films for sensing and security applications.

This work was supported by the AFOSR Young Investigator Program (Award No. FA9550-10-1-0226) and the National Science Foundation (Award No. 0925542 and the UMass Lowell GK-12 Waves and Vibes program). The authors would also like to thank James Ginn of Sandia National Laboratories for mid-IR ellipsometry measurements on the SOG used in this work.

[1] J. B. Pendry, D. Schurig, and D. R. Smith, Science **312**, 1780 (2006).
[2] D. Schurig, J. J. Mock, B. J. Justice, S. A. Cummer, J. B. Pendry, A. F. Starr, and D. R. Smith, Science **314**, 977 (2006).
[3] V. G. Veselago, Sov. Phys. Usp. **10**, 509 (1968).
[4] J. B. Pendry, Phys. Rev. Lett. **85**, 3966 (2000).
[5] A. Grbic and G. V. Eleftheriades, Phys. Rev. Lett. **92**, 117403 (2004).
[6] N. Fang, H. Lee, C. Sun, and X. Zhang, Science **308**, 534 (2005).
[7] J. J. Greffet and M. Nieto-Vesperinas, J. Opt. Soc. Am. A **15**, 2735 (1998).
[8] S. M. Rytov, Sov. Phys. JETP **2**, 466 (1955).
[9] N. Liu, M. Mesch, T. Weiss, M. Hentschel, and H. Giessen, Nano Lett. **10**, 2342 (2010).
[10] C. Wu, B. Neuner III, J. John, A. Milder, B. Zollars, S. Savoy, and G. Shvets, arXiv:1104.3129v1 (unpublished).
[11] S. O. C. Giraud and D. G. Hasko, Microelectron. Eng. **41–42**, 579 (1998).
[12] J. J. Greffet, R. Carminati, K. Joulain, J. P. Mulet, S. Mainguy, and Y. Chen, Nature (London) **416**, 61 (2002).
[13] J. A. Mason, D. C. Adams, Z. Johnson, S. Smith, A. W. Davis, and D. Wasserman, Opt. Express **18**, 25192 (2010).
[14] M. Diem, T. Koschny, and C. M. Soukoulis, Phys. Rev. B **79**, 033101 (2009).
[15] Y. Avitzour, Y. A. Urzhumov, and G. Shvets, Phys. Rev. B **79**, 045131 (2009).
[16] For details see COMSOL Multiphysics 3.5a User's Guide and RF Module User's Guide, www.comsol.com.
[17] S. Y. Lin, J. G. Fleming, and J. Moreno, Appl. Phys. Lett. **83**, 380 (2003).
[18] J. G. Fleming, Appl. Phys. Lett. **86**, 249902 (2005).